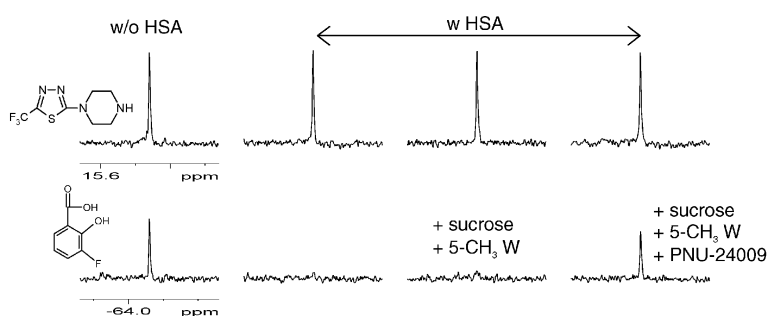Article

Fluorine-NMR Experiments for High-Throughput Screening: Theoretical Aspects, Practical Considerations, and Range of Applicability

Claudio Dalvit, Paul E. Fagerness, Daneen T. A. Hadden, Ronald W. Sarver, and Brian J. Stockman

More About This Article

Additional resources and features associated with this article are available within the HTML version:

- Supporting Information
- Links to the 8 articles that cite this article, as of the time of this article download
- Access to high resolution figures
- Links to articles and content related to this article
- Copyright permission to reproduce figures and/or text from this article

View the Full Text HTML

Fluorine-NMR Experiments for High-Throughput Screening: Theoretical Aspects, Practical Considerations, and Range of Applicability

Claudio Dalvit,*,[†] Paul E. Fagerness,[‡] Daneen T. A. Hadden,[§]
Ronald W. Sarver,[‡] and Brian J. Stockman[§]

*Contribution from the Chemistry Department, Pharmacia, Viale Pasteur 10,
20014 Nerviano (MI), Italy, and Analytical Chemistry and Structural and Computational
Chemistry, Pharmacia, 301 Henrietta Street, Kalamazoo, Michigan 49001*

Received February 13, 2003; E-mail: claudio.dalvit@pharmacia.com

Abstract: Competition ligand-based NMR screening experiments have recently been introduced to overcome most of the problems associated with traditional ligand-based NMR screening. Molecules with marginal solubility and high affinity for a given target can be easily identified in a high-throughput manner by screening chemical mixtures against the target in the presence of a weak- to medium-affinity ligand of known binding constant. While the original competition-based approaches utilized ^{1}H detection, significant advantages are obtained using ^{19}F detection. The absence of spectral overlap permits the screening of large chemical mixtures and allows for automated analysis of the spectra, even in the presence of protonated buffers, solvents, and detergents. The large chemical shift anisotropy of fluorine and the significant exchange contribution allow for the selection of a weak-affinity spy molecule, thus resulting in a lower binding affinity threshold for the identified NMR hits. The method, labeled FAXS (fluorine chemical shift anisotropy and exchange for screening) is rapid and requires only a limited amount of protein and, therefore, compares favorably with the other established non-NMR techniques used in high-throughput screening. Herein the theoretical aspects of this powerful ^{19}F-based approach are presented and discussed in detail. The experimental conditions together with the detection limits and binding constant measurements are investigated using human serum albumin as the target.

Introduction

Nuclear magnetic resonance is becoming increasingly important as a tool for the identification and optimization of molecules interacting with the receptor of interest. NMR has been known for a long time as a powerful method for studying interactions between a ligand and a macromolecule, including proteins and RNA or DNA fragments.[1] Recently the technique has been applied to the screening process within the pharmaceutical industry.[2-10] The low sensitivity of the technique together with

the requirement of a large amount of protein has limited its application to only some fortunate cases. Thanks to technological developments (e.g., cryoprobes and ultrahigh-field spectrometers) and some ligand-based NMR screening approaches,[11-17]

[†] Chemistry Department, Pharmacia, Italy.

[‡] Analytical Chemistry, Pharmacia, Michigan.

[§] Structural, and Computational Chemistry, Pharmacia, Michigan.

(1) (a) Roberts, G. C. K.; Jardetzky, O. *Adv. Protein Chem.* **1970**, *24*, 447–545. (b) Sheard, B.; Bradbury, E. M. *Prog. Biophys. Mol. Biol.* **1970**, *20*, 187–246.

(2) (a) Shuker, S. B.; Hajduk, P. J.; Meadows R. P.; Fesik, S. W. *Science* **1996**, *274*, 1531–1534. (b) Hajduk, P. J.; Sheppard, D. G.; Nettesheim, D. G.; Olejniczak, E. T.; Shuker, S. B.; Meadows, R. P.; Steinman, D. H.; Carrera, G. M., Jr.; Marcotte, P. M.; Severin, J.; Walter, K.; Smith, H.; Gubbins, E.; Simmer, R.; Holzman, T. F.; Morgan, D. W.; Davidsen, S. K.; Summers, J. B.; Fesik, S. W. *J. Am. Chem. Soc.* **1997**, *119*, 5818–5827.

(3) (a) Stockman, B. J. *Prog. Nucl. Magn. Reson. Spec.* **1998**, *33*, 109–151. (b) Stockman, B. J.; Farley, K. A.; Angwin, D. T. *Methods Enzymol.* **2001**, *338*, 230–246.

(4) Hajduk, P. J.; Meadows, R. P.; Fesik, S. W. *Q. Rev. Biophys.* **1999**, *32*, 211–240.

(5) (a) Moore, J. M. *Curr. Opin. Biotechnol.* **1999**, *10*, 54–58. (b) Peng, J. W.; Lepre, C. A.; Fejzo, J.; Abdul-Manan N.; Moore, J. M. *Methods Enzymol.* **2001**, *338*, 202–230.

(6) Diercks, T.; Coles, M.; Kessler, H. *Curr. Opin. Chem. Biol.* **2001**, *4*, 479–492.

(7) Pellecchia, M.; Sem, D. S.; Wüthrich, K. *Nat. Rev.* **2002**, *1*, 211–219.

(8) Van Dongen, M.; Weigelt, J.; Uppenberg, J.; Schultz, J.; Wikström, M. *Drug Discovery Today* **2002**, *7*, 471–478.

(9) Wyss, D. F.; McCoy, M. A.; Senior, M. M. *Curr. Opin. Drug Discovery Dev.* **2002**, *5*, 630–647.

(10) Stockman, B. J.; Dalvit C. *Prog. Nucl. Magn. Res. Spec.* **2002**, *41*, 187–231.

(11) (a) Meyer, B.; Weimar, T.; Peters, T. *Eur. J. Biochem.* **1997**, *246*, 705–709. (b) Henrichsen, D.; Ernst, B.; Magnani, J. L.; Wang, W.-T.; Meyer, B.; Peters, T. *Angew. Chem., Int. Ed.* **1999**, *38*, 98–102.

(12) Lin, M.; Shapiro, M. J.; Wareing, J. R. *J. Am. Chem. Soc.* **1997**, *119*, 5249–5250.

(13) Hajduk, P. J.; Olejniczak E. T.; Fesik, S. W. *J. Am. Chem. Soc.* **1997**, *119*, 12257–12261.

(14) (a) Chen, A.; Shapiro, M. J. *J. Am. Chem. Soc.* **1998**, *120*, 10258–10259. (b) Chen, A.; Shapiro, M. J. *J. Am. Chem. Soc.* **2000**, *122*, 414–415.

(15) (a) Mayer, M.; Meyer, B. *Angew. Chem., Int. Ed.* **1999**, *38*, 1784–1788. (b) Klein, J.; Meinecke, R.; Mayer, M.; Meyer, B. *J. Am. Chem. Soc.* **1999**, *121*, 5336–5337. (c) Mayer, M.; Meyer, B. *J. Am. Chem. Soc.* **2001**, *123*, 6108–6117.

(16) (a) Jahnke, W.; Perez, L. B.; Paris, C. G.; Strauss, A.; Fendrich, G.; Nalin, C. M. *J. Am. Chem. Soc.* **2000**, *122*, 7394–7395. (b) Jahnke, W.; Rüdisser, S.; Zurini, M. *J. Am. Chem. Soc.* **2001**, *123*, 3149–3150.

(17) (a) Dalvit, C.; Pevarello, P.; Tatò, M.; Veronesi, M.; Vulpetti, A.; Sundström, M. *J. Biomol. NMR* **2000**, *18*, 65–68. (b) Dalvit, C.; Fogliatto, G. P.; Stewart, A.; Veronesi, M.; Stockman, B. *J. Biomol. NMR* **2001**, *21*, 349–359.

it is now possible to screen large chemical mixtures in a short period of time. This has rapidly resulted in the successful and extensive application of NMR spectroscopy to numerous projects in the pharmaceutical industry and at universities.[18−22] The technique is used at all stages of drug discovery programs, including lead identification, lead validation, and lead optimization.

Although ligand-based NMR approaches are very powerful, they suffer from some drawbacks. Ligands that bind tightly to the receptor, ligands that have a slow kinetics, and ligands that bind covalently to the receptor cannot be detected. The competition ligand-based NMR screening experiments recently introduced[23−26] overcome all the problems associated with traditional ligand-based screening approaches. Molecules with marginal solubility and high affinity for the receptor of interest can also be easily identified with this method. The screening of chemical mixtures against the protein target is performed in the presence of a weak- to medium-affinity ligand of known binding constant referred to in this role as the spy molecule. Sometimes it is advantageous to perform the screening in the presence of an additional molecule, referred to in this role as the control molecule, that does not interact with the receptor.[10,24b,26] Both molecules are very soluble in order to avoid artifacts originating from nonspecific binding with the receptor or from interactions with the molecules of the mixture to be screened. The screening is performed simply by monitoring the relative intensities of the signals of the two molecules. Resonances from the actual molecules screened are not utilized.

The method, originally proposed with proton detection experiments, has recently been extended to fluorine detection experiments.[27] Since resonances from the actual molecules screened are not utilized, only the spy and control molecules are required to contain a fluoro moiety. This system of detection has some unique advantages. The absence of overlap permits the screening of large chemical mixtures and allows for automated analysis of the spectra. The large chemical shift anisotropy (CSA) of fluorine makes the difference in line width for the spy molecule in the free and bound state very large especially at the high magnetic fields currently used.[27,28] This

phenomenon combined with the large exchange contribution allows for the selection of a weak-affinity spy molecule, thus resulting in a lower binding affinity threshold for the identified NMR hits. The theoretical aspects of this powerful approach labeled FAXS (fluorine chemical shift anisotropy and exchange for screening) are presented and discussed in detail. The experimental conditions together with the detection limits and the binding constant measurements are investigated using human serum albumin (HSA) as test receptor.

Results and Discussion

Theory. The sensitivity of the ^{19}F NMR signal is proportional to $(\gamma_F/\gamma_H)^3$ where γ_F and γ_H are the gyromagnetic ratio of fluorine and hydrogen, respectively. Because ^{19}F is the only stable fluorine isotope and has spin 1/2, its sensitivity is high, i.e., 0.83 times that of the proton. Fluorine signals appear as singlet resonances in the presence of proton decoupling and are therefore intense.

The ^{19}F transverse relaxation represents an excellent parameter to be monitored for screening performed with competition binding experiments. The dipolar contributions to the line width of a fluorine or proton signal of a spy molecule are similar in magnitude. The transverse relaxation rate R_2 of the fluorine signal has an additional contribution originating from the large CSA interaction of the ^{19}F atom that is given by[29]

$$R_2^{CSA} = \frac{2}{15}\Delta\sigma^2\left(1 + \frac{\eta_{CSA}^2}{3}\right)B_0^2\gamma_F^2\tau_c\left\{\frac{2}{3} + \frac{1}{2(1 + \omega_F^2\tau_c^2)}\right\} \quad (1)$$

where $\Delta\sigma$ is the CSA of the ^{19}F atom and is given by $\Delta\sigma = \sigma_{zz} - (\sigma_{xx} + \sigma_{yy})/2$. The different σ's are the components of the chemical shift tensor. The asymmetry parameter $\eta_{CSA} = (3/2)(\sigma_{xx} - \sigma_{yy})/\Delta\sigma$, and for an axially symmetric chemical shift tensor $\eta_{CSA} = 0$. B_0 is the strength of the magnetic field, γ_F is the fluorine gyromagnetic ratio, ω_F is the fluorine Larmor frequency, and τ_c is the correlation time.

A simulation performed assuming an axially symmetric CSA tensor and assuming an equal CSA for the free and bound state of a ligand indicates that the difference in line width of the ^{19}F signal of the spy molecule between the free and bound state from just the CSA contribution alone can be very large.[27] This difference increases with the size of the receptor and with the square of the magnetic field strength. High magnetic fields can lead to extremely broad line widths (>200 Hz) for fluorine signals of either macromolecules (e.g., a protein selectively labeled with ^{19}F) or strongly protein-bound ligands.[28] Such line widths make the direct detection of fluorine resonances of the macromolecule or high-affinity ligands impractical for the purposes of screening. In contrast, the strong magnetic fields are particularly well-suited for competition binding experiments performed with a weak-affinity spy molecule where the population averaging between the free and bound states results in an observed line width that can be manipulated and monitored.[27]

(18) (a) Fejzo, J.; Lepre, C. A.; Peng, J. W.; Bemis, G. W.; Ajay, Murcko, M, A.; Moore, J. M. *Chem. Biol.* **1999**, *6*, 755−769. (b) Lepre C. A.; Peng, J.; Fejzo, J.; Abdul-Manan, N.; Pocas, J.; Jacobs, M.; Xie, X.; Moore, J. M. *Comb. Chem., HTS* **2002**, *5*, 583−590.

(19) (a) Hajduk, P. J.; Gerfin, T.; Böhlen J.-M.; Häberli, M.; Marek, D.; Fesik, S. W. *J. Med. Chem.* **1999**, *42*, 2315−2317. (b) Hajduk, P. J.; Burns, D. J. *Comb. Chem., High Throughput Screening* **2002**, *5*, 613−621. (c) Huth, J. R.; Sun, C. *Comb. Chem., High Throughput Screening* **2002**, *5*, 631−643.

(20) (a) Weigelt, J.; Van Dongen, M. J. P.; Uppenberg, J.; Schultz, J.; Wikström, M. *J. Am. Chem. Soc.* **2002**, *124*, 2446−2447. (b) Van Dongen, M. J. P.; Uppenberg, J.; Svensson, S.; Lundback, T.; Akerud, T.; Wikström, M.; Schultz, J. *J. Am. Chem. Soc.* **2002**, *124*, 11874−11880. (c) Weigelt, J.; Wikström, M.; Schultz, J.; Van Dongen, M. J. P. *Comb. Chem., High Throughput Screening* **2002**, *5*, 623−630.

(21) Pellecchia, M.; Meininger, D.; Dong, Q.; Chang, E.; Jack, R.; Sem, D. S. *J. Biomol. NMR* **2002**, *22*, 165−173.

(22) (a) Mayer, M.; James, T. L. *J. Am. Chem. Soc.* **2002**, *124*, 13376−13377. (b) Bernie, A. J.; Moser, R.; Bauml, E.; Blaas, D.; Peters, T. *J. Am. Chem. Soc.* **2003**, *125*, 14−15.

(23) Dalvit, C.; Fasolini, M.; Flocco, M.; Knapp, S.; Pevarello, P.; Veronesi, M. *J. Med. Chem.* **2002**, *45*, 2610−2614.

(24) (a) Dalvit, C.; Flocco, M.; Knapp, S.; Mostardini, M.; Perego, R.; Stockman, B. J.; Veronesi, M.; Varasi, M. *J. Am. Chem. Soc.* **2002**, *124*, 7702−7709. (b) Dalvit, C.; Flocco, M.; Stockman, B. J.; Veronesi, M. *Comb. Chem., High Throughput Screening* **2002**, *5*, 645−650.

(25) Jahnke, W.; Floersheim, P.; Ostermeier, C.; Zhang, X.; Hemmig, R.; Hurth, K.; Uzunov, D. P. *Angew. Chem., Int. Ed.* **2002**, *41*, 3420−3423.

(26) Siriwardena, A. H.; Tian, F.; Noble, S.; Prestegard, J. H. *Angew. Chem., Int. Ed.* **2002**, *41*, 3454−3457.

(27) Dalvit, C.; Flocco, M.; Veronesi, M.; Stockman, B. J. *Comb. Chem., High Throughput Screening* **2002**, *5*, 605−611.

(28) (a) Hull, W. E.; Sykes, B. D. *J. Mol. Biol.* **1975**, *98*, 121−153. (b) Gerig, J. T. *Methods Enzymol.* **1989**, *177*, 3−23. (c) Gerig, J. T. *Prog. NMR Spectrosc.* **1994**, *26*, 293−370.

(29) Canet, D. *Nuclear Magnetic Resonance Concepts and Methods*; John Wiley & Sons: Chichester, 1996.

The pulse sequences typically used employ a Carr−Purcell−Meiboom−Gill (CPMG) spin−echo scheme[30,31] before the acquisition period. The signal intensity of the spy molecule at the end of the spin−echo scheme $I_{(n2\tau)}$ is given by[32]

$$I_{(n2\tau)} = I_0 e^{-\gamma_F{}^2 G^2 D_{obs}(n2\tau)\tau^2/3} e^{-n2\tau R_{2,obs}} \qquad (2)$$

where I_0 is the signal intensity after the initial 90° pulse, 2τ is the interval between the train of 180° pulses, G represents the inhomogeneity of the static magnetic field, γ_F is the gyromagnetic ratio of fluorine, and n is the number of cycles of the spin−echo scheme. D_{obs}, the observed translation diffusion coefficient for the weak-affinity spy molecule, is given by the equation

$$D_{obs} = \frac{[EL]}{[L_{TOT}]} D_{bound} + \left(1 - \frac{[EL]}{[L_{TOT}]}\right) D_{free} \qquad (3)$$

where D_{bound} and D_{free} are the diffusion coefficients of the spy molecule in the bound and free states, respectively. $[EL]/[L_{TOT}]$ and $(1 - [EL]/[L_{TOT}])$ are the fraction of bound and free ligand, respectively.

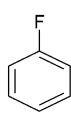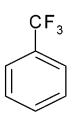$R_{2,obs}$, the transverse relaxation rate for the weak-affinity spy molecule, is given by the equation

$$R_{2,obs} = \frac{[EL]}{[L_{TOT}]} R_{2,bound} + \left(1 - \frac{[EL]}{[L_{TOT}]}\right) R_{2,free} +$$
$$\frac{[EL]}{[L_{TOT}]}\left(1 - \frac{[EL]}{[L_{TOT}]}\right) \frac{24\pi^2(\delta_{free} - \delta_{bound})^2}{K_{-1}} \qquad (4)$$

where $R_{2,bound}$ and $R_{2,free}$ are the transverse relaxation rate constants for the ligand in the bound and free states, respectively. The last term is the exchange term, where δ_{bound} and δ_{free} are the isotropic chemical shifts of the fluorine resonance of the spy molecule in the bound and free states, respectively and $1/K_{-1}$ is the residence time of the ligand bound to the protein. Equation 4 is valid only when the experiments are performed with a long 2τ period (where $\tau \gg 1/K_{-1}$). Experiments recorded with $\tau < 5/K_{-1}$ result in a reduced contribution of the exchange term to the observed transverse relaxation rate.[33]

Therefore screening is performed by using a long 2τ period. This is possible because the evolution under the heteronuclear ^1H−^{19}F scalar couplings is refocused at the end of the scheme. However, the 2τ period should not be very long in order to minimize signal attenuation originating from the spatial diffusion of the spy molecule (i.e., first exponential term of eq 2).

Selection of the Spy and Control Molecules. Table 1 reports the frequency of molecules containing a fluorine atom in three different commercially available chemical libraries. The table contains also the number of two substructures, monofluorobenzene and trifluoromethylbenzene, often used in our experiments. The large number of molecules containing a fluorine atom makes the selection of the spy and control molecules an easy task without recourse to chemical synthesis. An interesting feature

(30) Carr, H. Y.; Purcell, E. M. *Phys. Rev.* **1954**, *94*, 630−638.
(31) Meiboom S.; Gill, D. *Rev. Sci. Instrum.* **1958**, *29*, 688.
(32) Farrar T. C.; Becker, E. D. *Pulse and Fourier Transform NMR, Introduction to Theory and Methods*; Academic Press: New York, 1971.
(33) (a) Luz, Z.; Meiboom, S. *J. Chem. Phys.* **1963**, *39*, 366−370. (b) Allerhand, A.; Gutowsky, H. S. *J. Chem. Phys.* **1964**, *41*, 2115−2126.
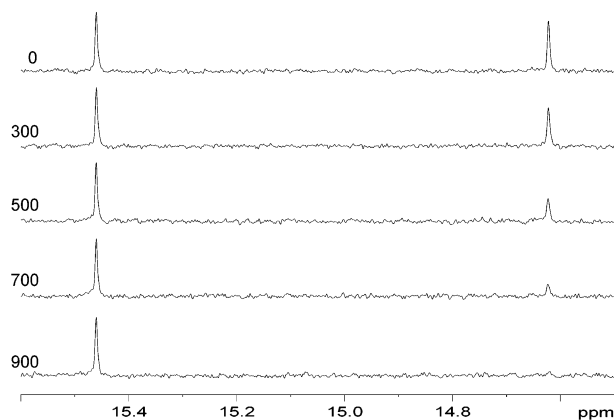
Table 1. Frequency of F-Containing Molecules in Different Commercially Available Libraries: ACD-SC (Available Chemical Directory of Screening Compounds), MDDR (MDL Drug Data Report), NCI (National Cancer Institute)

Compound Collection	molecules with F	F (phenyl)	CF₃ (phenyl)
ACD-SC	~12%	153K	43K
MDDR	~15%	11K	3K
NCI	~4%	3K	1K

emerging from Table 1 is the large number of fluorine-containing molecules present in the MDDR library. A chronological search within this library demonstrates that over the last 20 years the percentage of compounds in development containing at least one fluorine atom has doubled. A steady increase from 10.9% in the 1981−1985 period to 19.4% in the 1996−2000 period is observed. The fluorine atom has been increasingly introduced in the process of lead optimization for improving potency, physical−chemical properties, and metabolic stability against enzyme attack.

In the selection of the two molecules particular care should be given to their solubility since the presence of a fluorine atom increases the lipophilicity of a compound. Molecules that are not very soluble in aqueous solution are not suitable for screening experiments since they might bind in a nonspecific manner to the receptor. Therefore proton and fluorine spectra and proton WaterLOGSY spectra for the potential spy and control molecules are recorded in the absence of protein at a concentration typically 2−4 times higher (i.e., 100−200 μM) than the concentration used in the screening process. Only molecules that according to the NMR spectra are soluble and do not aggregate at these concentrations are considered as potential candidates for the spy and control molecules used for the screening.

A library of ^{19}F-containing molecules that fulfill the criteria described above has been generated in our laboratory. These molecules are tested in mixtures against the receptor with WaterLOGSY for the identification of a potential spy molecule. Other direct methods with ^1H or ^{19}F detection can also be used for this purpose. When possible, the X-ray structure of the spy molecule bound to the receptor is solved and/or a functional assay is performed. Both experiments are carried out at high spy molecule concentration due to the low affinity of the ligand. This is possible because the spy molecules were selected according to their high solubility in an aqueous solution. Although these experiments are not necessary for the screening, they can provide useful information concerning the binding site and the inhibitory activity.

Molecules with a CF₃ Group. Molecules containing a CF_3 group have the advantage of high sensitivity of the fluorine signal. Typical spin−echo ^{19}F spectra of the spy molecule 5-[1-methyl-3 (trifluoromethyl)-1*H*-pyrazol-5-yl]-2-thiophenecarboxylic acid (**1**) and control molecule 1-[5-(trifluoromethyl)1,3,4-

Figure 1. ^{19}F spin−echo spectra recorded as a function of the HSA concentration. The CF$_3$ resonance of the control molecule (**2**) is at +15.46 ppm, and the CF$_3$ resonance of the spy molecule (**1**) is at +14.62 ppm. The spectra were acquired with a total spin−echo period of 320 ms with an interval between the 180° pulses (2τ) of 40 ms. A total of 96 scans with a repetition time of 3.5 s and a spectral width of 25 ppm were acquired for each spectrum. The data were multiplied with an exponential function of 1 Hz before Fourier transformation. The concentration of the two molecules was 25 μM, whereas the concentration for HSA was, from top to bottom, 0, 300, 500, 700, and 900 nM. The signal intensity ratio $I(\mathbf{1})/I(\mathbf{2})$ is, from top to bottom, 0.86, 0.66, 0.38, 0.21, and 0.07.

thiadiazol-2-yl]piperazine (**2**) recorded with proton decoupling during the acquisition period in the presence of different concentrations of HSA are shown in Figure 1. ITC measurements performed with **2** did not find any evidence of binding

(1)   **(2)**
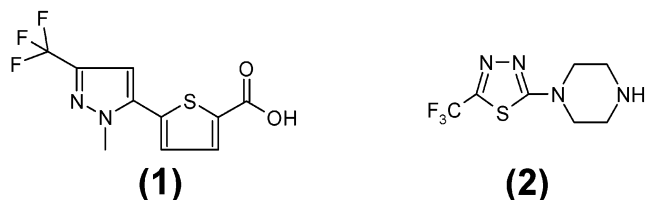
to HSA (only heat of dilution was detected with 8 μL injections of 800 μM of **2** into 30 μM HSA) in agreement with the NMR results. A concentration of only 25 μM for both molecules was used in the NMR experiments. The low concentration of the spy molecule avoids problems arising from nonspecific binding and aggregation. Disadvantages with these molecules are represented by the rapid rotation of the fluorine atoms about the C_3 axis of the group observed even in the bound state. This results in a limited difference in line width for the CF$_3$ signal of the spy molecule between the free and bound state. However the exchange contribution to the line width can be large.

Molecules with a CF Group. Molecules with a CF group are particularly suited for the competition ligand based screening experiments. The ^{19}F CSA can be very large therefore increasing the difference in line width between the free and bound state of the spy molecule according to eq 1. For example the CSA for an aromatic CF ranges from 71 ppm for monofluoro-benzene to 158 ppm for hexafluoro-benzene.[34] In addition, the ^{19}F CSA of the spy molecule in the bound state can increase from an "ortho effect" or from the direct involvement of the fluorine atom in an hydrogen bond with the protein. These two phenomena also have the effect of rendering a large difference in the isotropical chemical shift for the free and bound state.
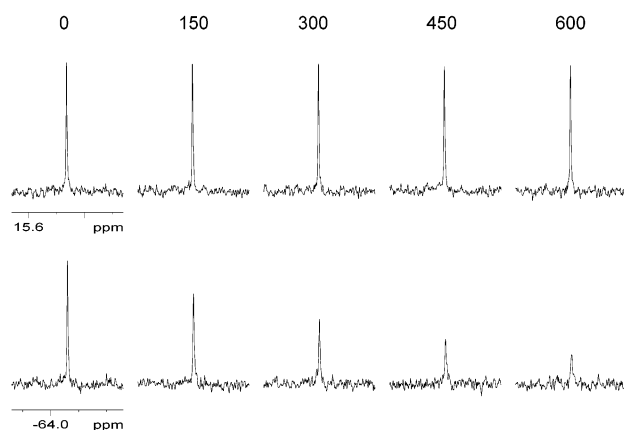
(34) Raber, H.; Mehring M. *Chem. Phys.* **1977**, *26*, 123−130.

Figure 2. ^{19}F spin−echo spectra recorded as a function of the HSA concentration. The CF resonance of the spy molecule (**3**) is at −64.06 ppm (lower spectra), and the CF$_3$ resonance of the control molecule (**2**) is at +15.46 ppm (upper spectra). The spectra were acquired with a total spin−echo period of 80 ms with an interval between the 180° pulses (2τ) of 40 ms. A total of 96 scans were recorded for the lower spectra and 64 scans for the upper spectra with a repetition time of 3.5 s and a spectral width of 25 ppm were acquired. The data were multiplied with an exponential function of 1 Hz before Fourier transformation. The concentration of **3** and **2** was 50 and 25 μM, respectively, whereas the concentration for HSA was, from left to right, 0, 150, 300, 450, and 600 nM. The signal intensity ratio $I(\mathbf{3})/I(\mathbf{2})$ at the plotted scale intensity is, from left to right, 0.94, 0.69, 0.53, 0.36, and 0.25.

For a weak affinity ligand the exchange term of eq 4 can contribute significantly to the line width of the spy molecule in the presence of the protein. The fluorine signal is usually scalar coupled with several protons and therefore for sensitivity improvement it is necessary to record the spectra with proton decoupling during acquisition. Figure 2 shows typical spin−echo fluorine spectra for the spy molecule 2-hydroxy 3-fluorobenzoic acid (**3**) and control molecule (**2**) recorded with proton

(3)
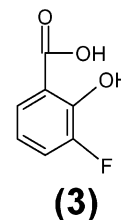
decoupling as a function of HSA concentration. A drawback with these molecules is the required higher concentration for the experiments. The spectra of Figure 4 were recorded with a concentration for the spy molecule of 50 μM.

Titration and Screening Experiments. After the selection of the spy and control molecules, titration experiments as a function of the protein concentration are recorded as shown in Figures 1 and 2. The intensity ratio of the two fluorine signals is plotted as a function of the fraction of protein-bound spy molecule as shown in the example of Figure 3. The fraction of bound compound is calculated by using the dissociation binding constant derived from other techniques (e.g., ITC or fluorescence spectroscopy) as previously described.[24a,b] These techniques also provide the number of binding sites (n) for the spy molecule, a parameter that is very important for the competition binding experiments. ITC measurements provided an n value that is close to 4 for **1** and close to 1 for **3**. Therefore, although molecule **1** can still be used for screening purposes with some limitations in the interpretation of the experimental results, it cannot be
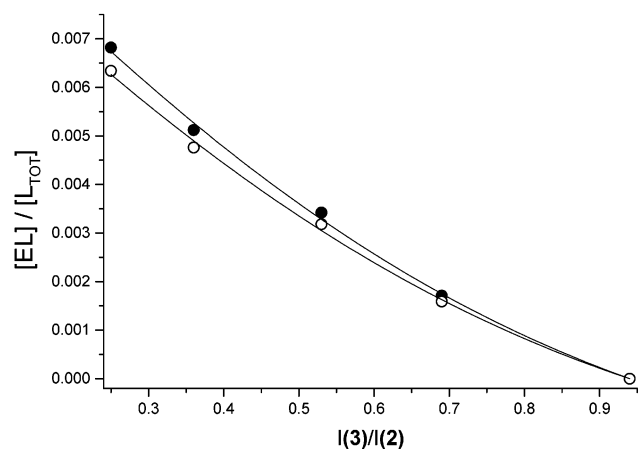
Figure 3. Plot of the signal intensity ratio (*x* axis) of the two ^{19}F signals of Figure 2 as a function of the fraction of bound spy molecule ([EL]/[L$_{TOT}$]) (*y* axis). The last point on the right corresponds to the value in the absence of the protein. Two ratios ([EL]/[L$_{TOT}$]) were calculated as previously described using the limits of the ITC-derived K_D value of 41 ± 3.3 μM for **3**. Values indicated by open circles were calculated with a K_D of 44.3 μM; values indicated by filled circles were calculated with a K_D of 37.7 μM. The curves represent the best fits of the experimental points.

used for deriving the binding constants of the NMR hits. Molecule **3** represents a suitable spy molecule since it has only one binding site on HSA at the concentration used in our experiments. According to its chemical structure, an aspirin analogue, its putative binding site would be the Sudlow site I (located in subdomain IIA).[35] Two different values for the fraction of protein-bound spy molecule **3** are used in Figure 3 using the two limit values of K_D determined by the experimental error. In our specific case, the ITC derived K_D for **3** was 41 ± 3.3 μM, and thus the two limit values of K_D correspond to 37.7 and 44.3 μM, respectively.

It should be pointed out that the NMR experiments could also be recorded in the presence of only the spy molecule.[27] In this case, however, two experiments have to be recorded: one without the CPMG sequence (i.e., $2n\tau = 0$) and another with a CPMG with a long $2n\tau$. The signal intensity ratio extracted from these two spectra is then plotted as a function of the fraction of bound spy molecule.

The graphs of Figure 3 are then used for setting up the experimental conditions necessary for FAXS. Figure 4 shows the screening process performed against HSA with **3** as spy molecule. For screening, a total spin−echo period ($2n\tau$) was selected for which the signal of the spy molecule is approaching zero. The presence in the mixture of 5-CH$_3$ D,L Trp and sucrose (third spectra from left), known as nonbinders, does not alter the spectrum of the spy molecule. In contrast, the presence in the mixture of the warfarin derivative 4-hydroxy-3-[1-(*p*-iodophenyl)-3-oxobutyl]coumarin (**4**) (right) results in the reappearance of the signal of **3**. This results, according to the
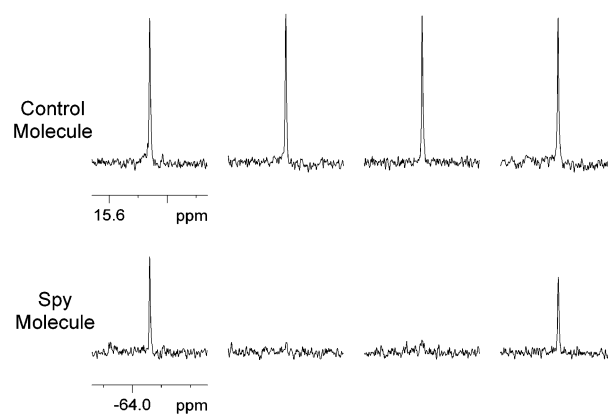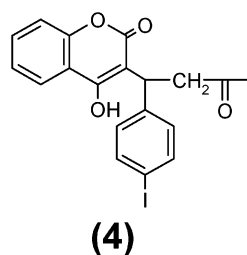

(4)

Figure 4. ^{19}F NMR ligand-based competition binding screening performed with the control molecule (**2**) (top) and the spy molecule (**3**) (bottom). The spectra were recorded with a total spin−echo period of 160 ms with an interval between the 180° pulses (2τ) of 40 ms. A total of 96 scans were recorded with a repetition time of 3.5 s and a spectral width of 25 ppm. The data were multiplied with an exponential function of 1 Hz before Fourier transformation. The concentration of **3** and **2** was 50 and 25 μM, respectively. The spectra on the left were recorded in the absence of protein, while all other spectra were recorded in the presence of 600 nM HSA. The latter were recorded in the absence of a chemical mixture (second from left), in the presence of 50 μM 5-CH$_3$ D,L Trp and sucrose (third from left), and in the presence of 50 μM 5-CH$_3$ D,L Trp, sucrose, and 25 μM **4** (right).

graphs of Figure 3, from the displacement of the spy compound from the protein. The extent of displacement can then be used to calculate rapidly the binding constant of the NMR hit,[24a,b] as described in Table 2. To derive a reliable value for the binding constant, one also has to record the proton spectrum. This is necessary for calculating the concentration of the NMR hit by simply comparing the integral of a signal of the spy molecule for which the concentration is known with the integral of a signal of the NMR hit. The NMR-derived K_D for **4** compares favorably with the value derived from a full titration fluorescence measurement. Since its first application,[24a] we have now calculated binding constants using this approach for several hundred compounds with K_D values ranging from a few nM to high μM. For a pure competition binding mechanism and a single binding site, excellent agreement was observed between the single-point NMR-derived binding constants and the full titration fluorescence- and ITC-derived binding constants. This NMR approach also allows the determination of high-affinity binding constants that would not be easily obtained with other NMR methods.

Limit of Detection. Owing to the large CSA and the large exchange contribution for a weak binding affinity molecule, it is possible to significantly reduce the concentration of protein needed for FAXS. This can be appreciated in Figure 5, where the screening is performed with **3** in the presence of HSA at a concentration of only 150 nM. Despite the large ratio [L$_{TOT}$]/[E$_{TOT}$] (=330) and the small ratio [EL]/[L$_{TOT}$] (=0.00165 using the K_D of 41 μM), it is possible to observe the effect of the small fraction of bound ligand (only 1 bound molecule for 606 free molecules) and perform the screening at such low protein concentrations. This could represent at a first analysis as a fortunate case. According to solid state NMR work, the presence of an OH group in the ortho position is responsible for a shift of 50 ppm in the component of the chemical shift tensor

(35) Theodore, P., Jr. *All about Albumin Biochemistry, Genetics, and Medical Applications*; Academic Press: San Diego, 1996.

Table 2. Single-Point NMR-Derived Binding Constant for **4** and Its Comparison with Measured Fluorescence Value[a]

$I(3)/I(2)$	K_D	[I]	$[L_{TOT}]$	$[E_{TOT}]$	$[EL]/[L_{TOT}]$	[EL]	K_D^{app}	K_I^{NMR}	K_I^{fluo}
0.698	44.3	25	50	0.6	0.00159	0.080	326.8	3.9 ± 0.9	3.3 ± 0.3
0.698	37.7	25	50	0.6	0.00171	0.086	300.4	3.6 ± 0.8	

[a] All values for the concentration and binding constants are expressed in μM. K_D is the binding constant of **3** derived from ITC, and K_I^{fluo} is the binding constant for **4** derived from fluorescence. [I], $[L_{TOT}]$, and $[E_{TOT}]$ are the concentration of **4**, **3**, and HSA, respectively. The K_I^{NMR} is the binding constant for **4** derived from the NMR measurements as previously described.[24a,b] The error of the K_I^{NMR} is due to an estimated $\pm5\%$ error in the signal intensity ratio measurement.
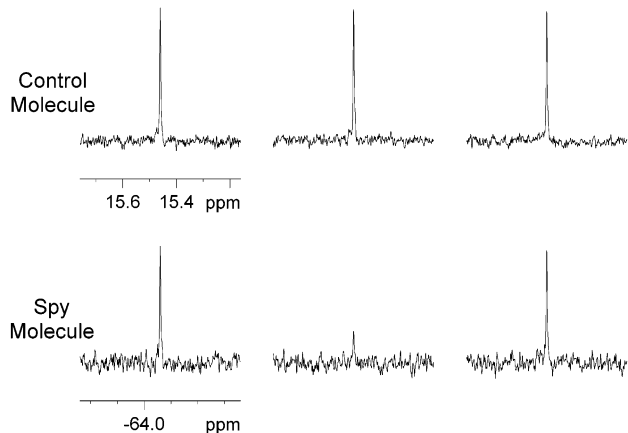

Figure 5. Detection limits of FAXS. Experiments performed with the control molecule (**2**) (top) and the spy molecule (**3**). The spectra were recorded with a total spin−echo period of 320 ms (top) and 1.2 s (bottom) with an interval between the 180° pulses (2τ) of 40 ms. A total of 64 (top) and 128 (bottom) scans were recorded with a repetition time of 3.5 s and a spectral width of 25 ppm. The data were multiplied with an exponential function of 1 Hz before Fourier transformation. The concentration of **3** and **2** was 50 and 25 μM, respectively. The spectra on the left were recorded in the absence of protein, while all other spectra were recorded in the presence of only 150 nM HSA. The latter were recorded in the absence of a chemical mixture (second from left) and in the presence of a mixture containing 25 μM **4** (right).

perpendicular to the aromatic ring, thus resulting in a large ^{19}F CSA.[34] However, we were also able to observe similar behavior with other proteins and with molecules containing a para-fluoro benzyl moiety (data not shown). The explanation of the sensitivity of the method is likely due to the large contribution of the exchange term to the observed transverse relaxation. This can be appreciated in the simulation of Figure 6. The simulations for R_2 (the transverse relaxation rate of the spy molecule signal due to exchange contribution and relaxation rate of the bound state) was performed using the Swift and Connick equation:[36]

$$R_2 = \frac{[EL]}{[L_{TOT}]\tau_{res}}$$
$$\left[\frac{R_{2,bound}\left(R_{2,bound} + \dfrac{1}{\tau_{res}}\right) + 4\pi^2(\delta_{free} - \delta_{bound})^2}{\left(R_{2,bound} + \dfrac{1}{\tau_{res}}\right)^2 + 4\pi^2(\delta_{free} - \delta_{bound})^2} \right] \quad (5)$$

where τ_{res} is the residence time of the spy molecule bound to the protein. The term proportional to the effective field is not contained in eq 5 because it is small due to the long τ period used in our NMR screening experiments. The two simulations were performed with $[EL]/[L_{TOT}]$ (= 0.00165, i.e., our extreme example) and $[EL]/L_{TOT}$ (= 0.02, i.e., a typical experimental condition used in NMR screening). For the simulation we have
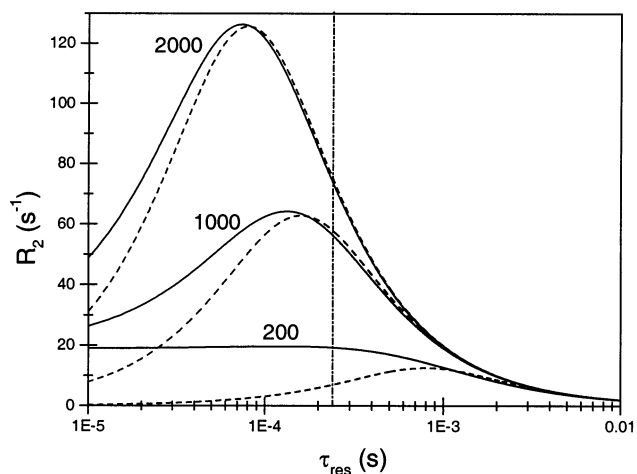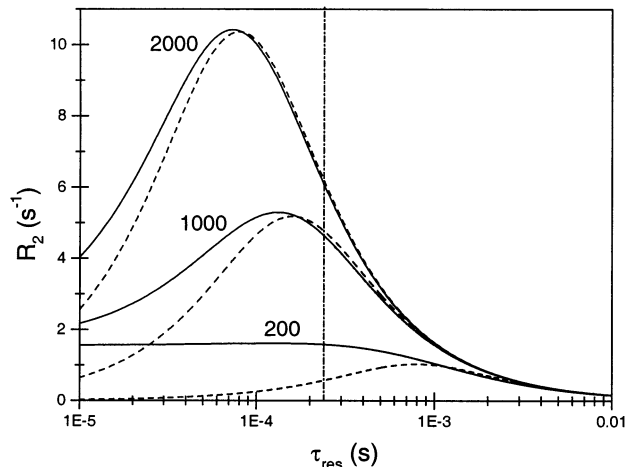
(36) Swift, T. J.; Connick, R. E. *J. Chem. Phys.* **1962**, *37*, 307−320.

Figure 6. Transverse relaxation of the spy molecule ^{19}F signal due to the exchange between free and bound state with (continuous line) and without (dashed line) contribution from $R_{2,bound}$ as a function of τ_{res}. The simulations were performed with eq 5 using three different ($\delta_{free} - \delta_{bound}$) (values in Hz indicated with the curves). A ^{19}F linewidth for the bound state of 300 Hz was used for the simulation with $R_{2,bound}$ contribution. The simulations were carried out with a fraction of bound spy molecule $[EL]/[L_{TOT}]$ of 0.00165 (upper graph) and 0.02 (lower graph). The dashed-dotted vertical line is drawn at τ_{res} of 2.4×10^{-4} s which represents an approximate τ_{res} for **3** in the assumption of an on-rate, K_{on} of 1×10^8 M^{-1} s^{-1}.

considered three chemical shift differences for the ^{19}F resonance of the spy molecule. Two simulations were performed in the presence of exchange with and without $R_{2,bound}$ contribution. This was necessary in order to make the comparison of the relative contribution of the exchange term and $R_{2,bound}$ to the linewidth of the spy molecule signal. It is evident from the graphs of Figure 6 that the exchange contribution can be significant even at very low fraction of bound spy molecule when the difference in chemical shift is large. The ($\delta_{free} - \delta_{bound}$) term can be large (up to several ppm) for the ^{19}F signal of a ligand and therefore the exchange contribution is substantial

for τ_{res} in the range of 10^{-5} to 10^{-3} s, i.e., a typical value for a weak affinity ligand. A τ_{res} of 2.4×10^{-4} s (dashed-dotted vertical line in Figure 6) for **3** is obtained using an approximate on-rate $K_{on} = 1 \times 10^{8}$ M^{-1} s^{-1} (reasonable value for diffusion-limited binding) and the determined K_D of 41 μM. This time interval is in the time region where significant broadening is predicted. It should be pointed out that the exchange term does not depend on the correlation time of the protein, and therefore the ^{19}F competition binding experiments can also be applied to the screening against small proteins. It is evident in Figure 6 that on the right of the maxima (slow exchange region) there is no contribution from $R_{2,bound}$ to the observed linewidth of the spy molecule signal. An $R_{2,bound}$ effect is observed on the left of the maxima (fast exchange region) reaching the maximum contribution value of $([EL]/[L_{TOT}])R_{2,bound}$ as also described by eq 4. The simulations of Figure 6 clearly demonstrate the sensitivity of the method that allows the use of very low concentrated protein. It is expected that working at higher magnetic fields will further improve the performance of the method due to the higher sensitivity and more pronounced effect of CSA and exchange to the transverse relaxation of the ^{19}F signal of the spy molecule. Protein concentrations as low as 50 nM could then be used with FAXS. An additional reduction in protein concentration could be achieved with the use of cryoprobe technology optimized for ^{19}F detection. This will allow screening of a large number of molecules against proteins that cannot be expressed in high amount (e.g., membrane proteins).

Throughput. The spectra reported in Figure 5 were recorded with 128 scans and a total measuring time of 10 min. Fluorine spectra can be recorded very rapidly with a cryoprobe. A conservative estimate of a 2-fold sensitivity improvement with cryoprobe technology would translate into a 4-fold reduction in acquisition time. Therefore the spectra of Figure 5 could have been recorded in just 150 s, thus enhancing the throughput of this screening process. It should be pointed out that problems of radiation damping encountered in proton-detected experiments recorded with cryoprobes are absent in the fluorine-detected experiments because of the low concentration of the spy and control molecules.

Compounds are typically screened in small mixtures with concentration similar to the concentration of the weak-affinity spy molecule. This screening approach allows identification of ligands that have an affinity for the receptor similar or stronger than the affinity of the spy molecule. A typical range for the K_D of the spy molecule is between a few dozen μM to a few hundred μM. However, if the main goal is the identification of only high- and medium-affinity ligands, it is possible to perform the screening using large mixtures ($\geq$100 molecules). A low concentration for a high or medium affinity competing molecule is sufficient to displace the weak affinity spy molecule. Therefore this low concentration allows for the preparation of large chemical mixtures without experiencing severe problems of aggregation and solubility. The use of large mixtures reduces the measuring time and the protein consumption. Screening of large mixtures is possible also because of the absence of spectral overlap with the ^{19}F signals of the spy and control molecules. The likelihood of overlap in the presence of some fluorine-containing molecules represents an extremely rare event due to the limited number of sharp singlet ^{19}F signals (fluorine-
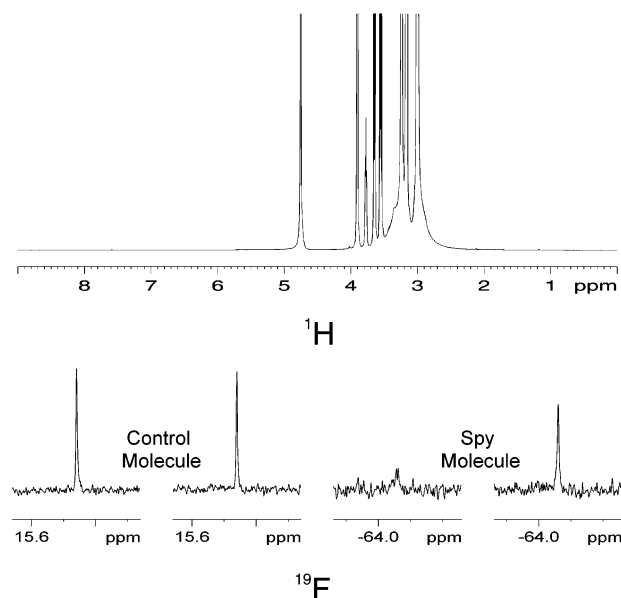

Figure 7. FAXS performed in the presence of nondeuterated buffers and detergents. (Top) Proton spectrum of a 600 nM solution of HSA in 100 mM HEPES and 1% glycerol and in the presence of 50 μM of the spy molecule (**3**) and 25 μM of the control molecule (**2**). After water suppression the only visible signals are those of the buffer and glycerol. A total of 128 scans were recorded with a repetition time of 2.7 s. (Bottom) ^{19}F spectra recorded for the same solution in the absence (first and third spectra from left) and in the presence (second and fourth spectra from left) of a mixture containing 25 μM **4**. The spectra were recorded with a total spin−echo period of 160 ms with an interval between the 180° pulses (2τ) of 40 ms. A total of 64 (left) and 128 (right) scans were recorded with a repetition time of 3.5 s and a spectral width of 25 ppm. The data were multiplied with an exponential function of 1 Hz before Fourier transformation.

containing molecules typically have only one CF or CF$_3$ group) and due to the large dispersion of ^{19}F chemical shift.

However, the deconvolution process of large mixtures can become lengthy. A possible strategy for speeding up this process, when the X-ray structure or a 3D homology model of the receptor is known, is the use of in-silico docking tools. The compounds of the active mixtures could be docked against the receptor and ranked according to their interaction energy. The best scoring molecules would then be selected and tested as single molecules or in small mixtures using FAXS. This procedure could result in the rapid identification of the active molecules present in the large mixtures.

Screening in the Presence of Protonated Solvents and Detergents. A particular advantage of the ^{19}F ligand-based competition binding experiments is the possibility to perform the screening even in the presence of protonated solvents, buffers, or detergents. The proton spectrum of HSA in the presence of 100 mM HEPES and 1% glycerol is shown in Figure 7. The intense signals of the buffer and glycerol mask the observation of the weak signals of the spy and control molecules necessary for performing the screening. These problems are not encountered in the ^{19}F detection experiments. Therefore it is possible to perform FAXS as shown in Figure 7 even in these difficult experimental conditions. Because of these properties, fluorine ligand-based competition binding screening experiments are particularly advantageous to the screening of molecules against membrane proteins dissolved in SDS or other detergents. Once a suitable spy molecule has been identified, the FAXS will provide reliable hits. Molecules that simply bind to the

membranes and/or detergents and that appear as potential ligands in other types of assays will not be detected in the ^{19}F experiments described here. Only molecules that compete with the spy molecule are identified. Finally, the experiments can also be used for screening plant and fungi extracts and for screening molecules within living cells.

Conclusion

The ^{19}F experiments performed with a weak-affinity ligand represent a powerful and sensitive NMR approach for primary screening of compounds binding to the target of interest, including proteins and DNA or RNA fragments. Since resonances from the actual molecules screened are not utilized, only the spy and control molecules are required to contain a fluoro moiety. Thus, FAXS should find numerous uses in the pharmaceutical industry and should further extend the impact of NMR-based screening on the drug discovery process. The method is rapid and requires only a limited amount of protein and therefore compares favorably with the other established non-NMR techniques used in high-throughput screening. In addition, the method provides within a single experiment a meaningful value for the binding constant of the NMR hit. The absence of overlap permits screening of large chemical mixtures originating from combinatorial chemistry, medicinal chemistry, or natural product extraction. Screening against membrane proteins dissolved in different detergents is also possible with this approach. Finally, it is envisioned that these experiments can be extended to the screening of molecules against a receptor located within living cells.

Material and Methods

Fatty acid free human serum albumin (A-3782) was purchased from Sigma and used without further purification. The NMR samples, with the exception of the sample used for the experiments of Figure 7, were in phosphate-buffered saline (PBS, code: P-3813, Lot 100K8211 from Sigma) pH 7.4 in the presence of 5 μM EDTA. D$_2$O was added to the solution (8% final concentration) for the lock signal. The small molecules were prepared in concentrated stock solutions in either deuterated DMSO or water and stored at 253 K.

NMR. All NMR spectra were recorded at 300 K with a Bruker Avance 600 NMR spectrometer operating at a ^{19}F Larmor frequency of 564 MHz. A dual coil {^{19}F}−{^{1}H} probe was used with the inner coil tuned to ^{19}F and the outer coil tuned to ^{1}H frequency. The fluorine background of these probes does not interfere with the measurements.

These signals are broad and therefore are not visible in the spectra of the spy and control molecule recorded with a spin−echo scheme. All the spectra were recorded with a weak Waltz-16 proton decoupling[37] applied during the acquisition period. Typically 4−8 dummy scans were recorded for temperature equilibration. Carr−Purcell−Meibom−Gill schemes of different length and long 2τ interval were used before the acquisition period. Chemical shifts were referenced to trifluoroacetic acid.

Fluorescence. Fluorescence measurements were acquired on a Jasco J-715 spectropolarimeter using an auxiliary photomultiplier tube positioned perpendicular to the excitation beam. The excitation wavelength was 310 nm (with a 5 nm bandwidth), and a 385 nm cutoff filter was employed. Affinity measurements were made using the same source of fatty acid-free HSA as used for NMR experiments. Analyte and HSA solutions were prepared in phosphate-buffered saline (PBS, code: P-3813, Lot 100K8211 from Sigma) pH 7.4 in the presence of 5 μM EDTA. The buffer was filtered through a 0.2 μm filter prior to use. Albumin affinity was determined by aliquoting 2.0 mL of a 3 μM solution of analyte into a quartz cuvette, path length of 1.0 cm, and titrating the solution with HSA (stock concentration of 250 μM).

ITC. Isothermal titration calorimetry experiments were performed using an OMEGA titrating microcalorimeter from Microcal, Inc. (Northampton, MA). The titrating microcalorimeter consisted of a sample and reference cell held in an adiabatic enclosure. The reference cell was filled with PBS. A 23 μM solution of HSA in PBS +2% DMSO was placed in the 1.37 mL sample cell. Analyte at 0.8 mM in the same buffer was held in a 250 μL syringe. Thirty injections (8 μL each and 12 s/inj.) of analyte were made by a computer-controlled stepper motor into the sample cell held at 25 °C. The syringe stir rate was 400 rpm. Heat absorbed or released with each injection was measured by a thermoelectric device connected to a Microcal nanovolt preamplifier. Titration isotherms for the binding interactions were comprised of the differential heat flow for each injection. Heat of dilution obtained by injecting analyte into PBS was negligible. Binding isotherms were fit to a single binding site model[38] using an iterative nonlinear least-squares algorithm included with the instrument.

(37) Shaka, A. J.; Keeler, J.; Freeman, R. *J. Magn. Reson.* **1983**, *53*, 313−340.
(38) Wiseman, T.; Williston, S.; Brandts, J. F.; Lin L. *Anal. Biochem.* **1989**, *179*, 131−137.